



Vacuum Chambers and NEG Coating Technologies

Alexander Krasnov

Budker Institute of Nuclear Physics (BINP), Novosibirsk, Russia

E-mail address: a.a.krasnov@inp.nsk.su

- **Dynamic gas density**
- **Role of surface and radiation**
- **Cold beam pipe. Hydrogen accumulation**
- **Other requirements for vacuum beam pipe**
- **LHC arc beam pipe**
- **Equations for residual dynamic gas density prediction**
- **Surface Conditioning**
- **Solutions made for LHC arc beam pipe**

- **NEG coating**
- **Example: PETRA III DWG**

Very interesting but not in the presentation:

SuperKEKB solutions for EC mitigation, HF impedance

XFEL impedance budget. Technical solutions

MAX IV SR Source

NEG characterization at BINP

BINP technologies for vacuum chamber fabrication

Vacuum requirements

Residual gas density should be at level $10^5 \div 10^9 \text{ cm}^{-3}$ (pressure $4 \cdot 10^{-10} \div 4 \cdot 10^{-6} \text{ Pa}$ at RT)

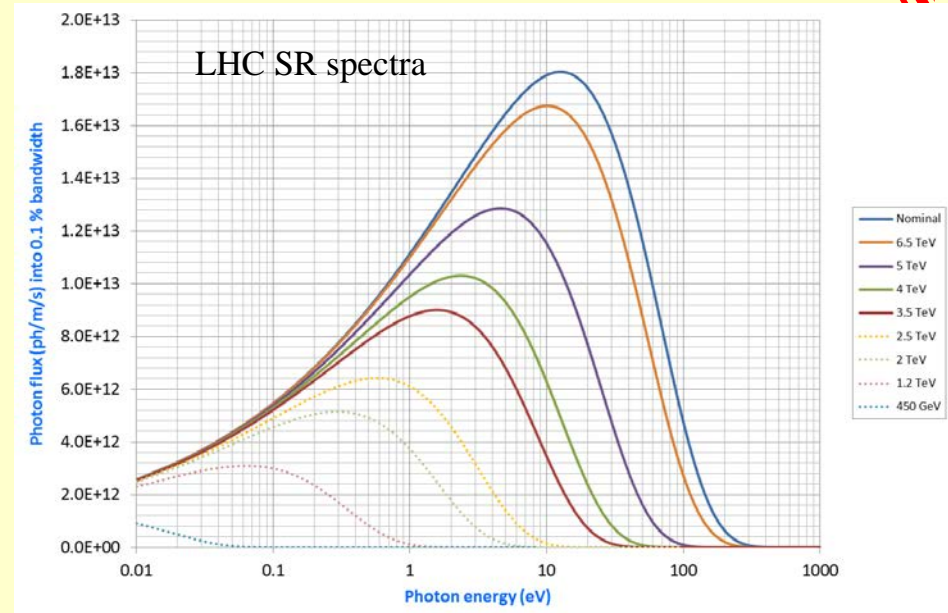
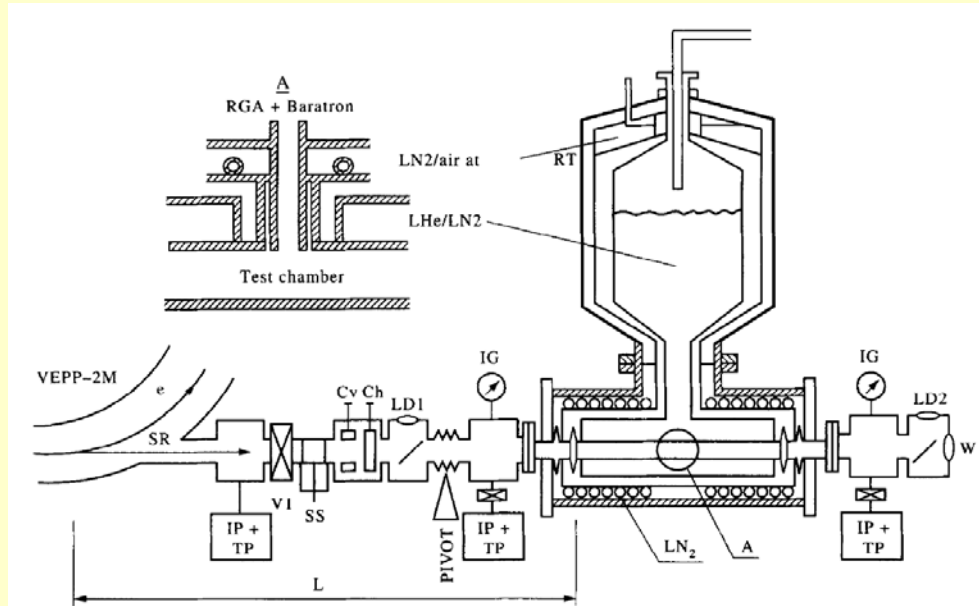
Metallic surface contains $10 \div 100 \text{ ML}$ ($1 \text{ ML} \approx 10^{15} \text{ cm}^{-2}$) of

- Chemically bound: MxOy , Mx(OH)y , $\text{Mx(HOC}_3\text{)}_y$, carbon clusters
- Physically adsorbed: H_2O , organics

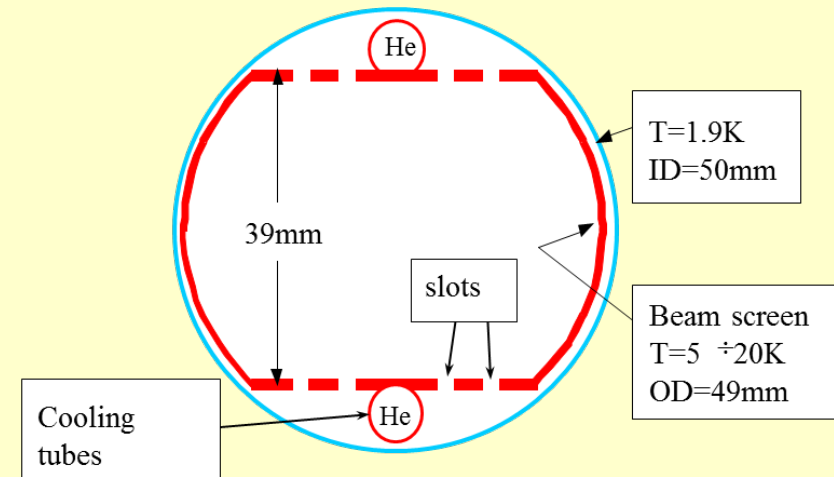
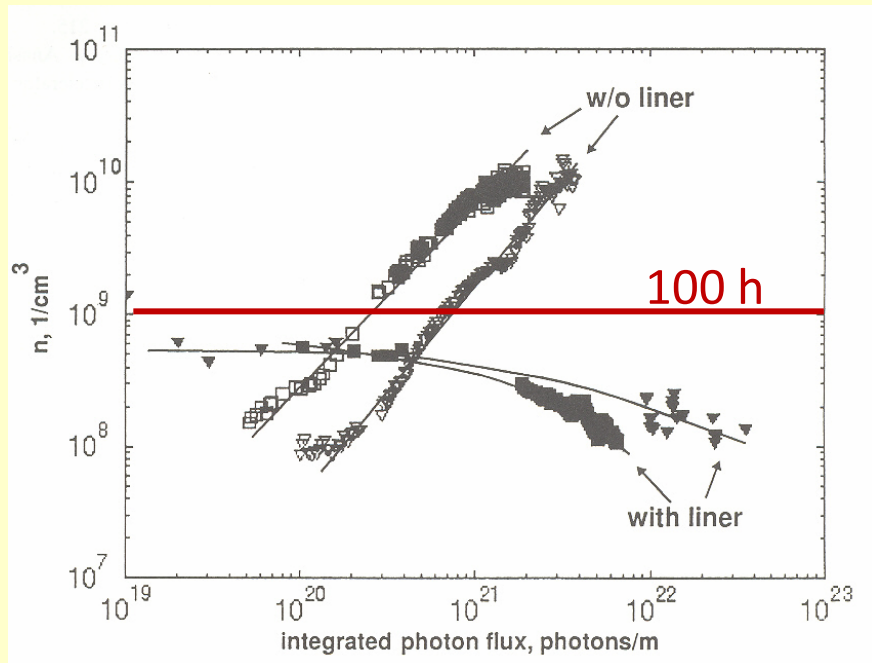
Example: Surface of a tube with $D=5 \text{ cm}$ contains on $10^7 \div 10^8$ times more molecules than ones inside the tube in gas phase at density 10^9 cm^{-3} !

Radiation can provoke dissociation of the molecules which causes desorption of:

- H_2 - most critical for cryogenic beam pipe because H_2 can re-desorb on surface with very low binding energy
- CO , CO_2
- Saturated hydrocarbons CxHy (due to catalytic reactions on surface)



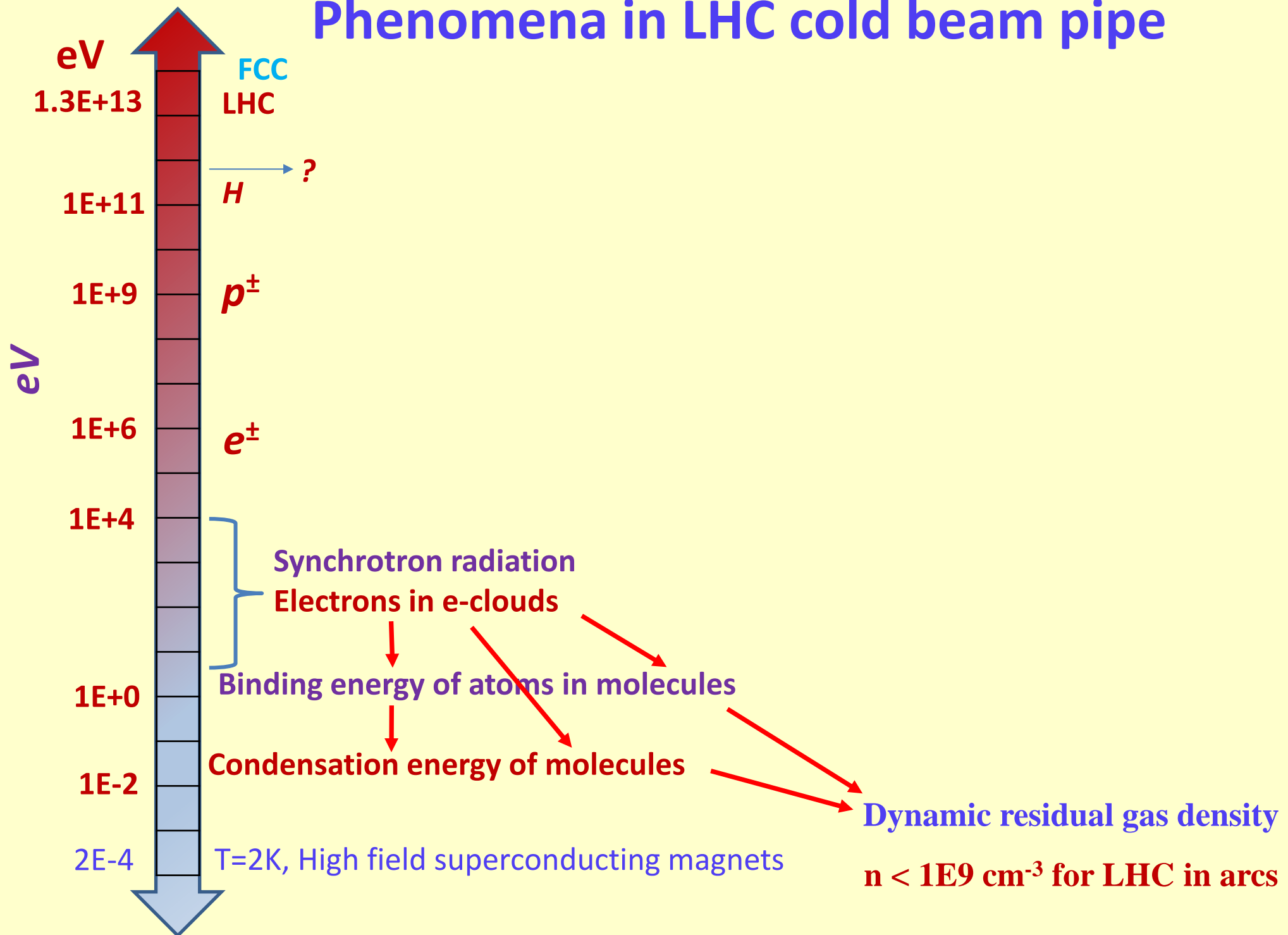
Experiments at BINP (25 years ago!) in collaboration with SSC (20 TeV per beam) and CERN vacuum groups



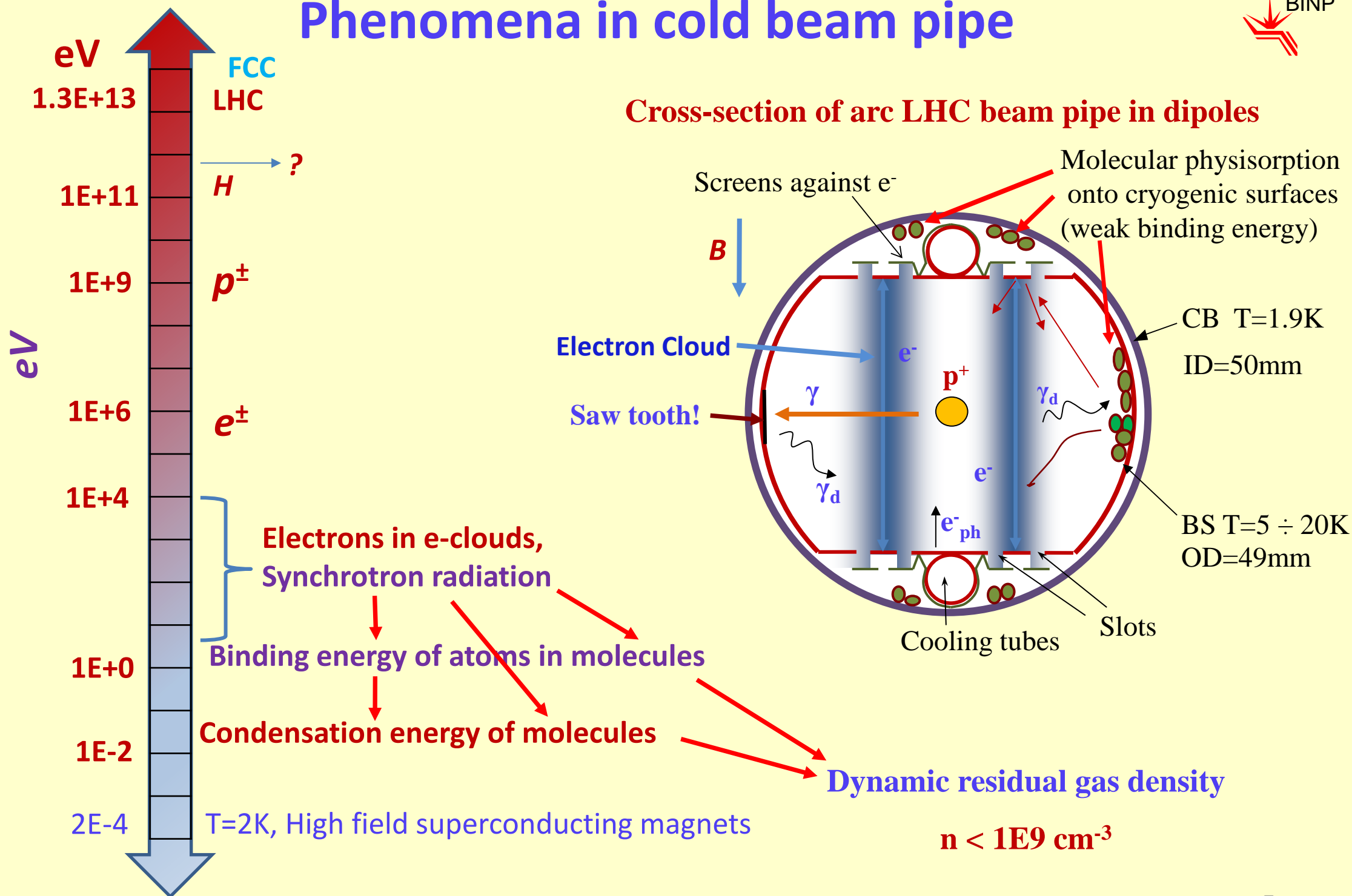
Other requirements

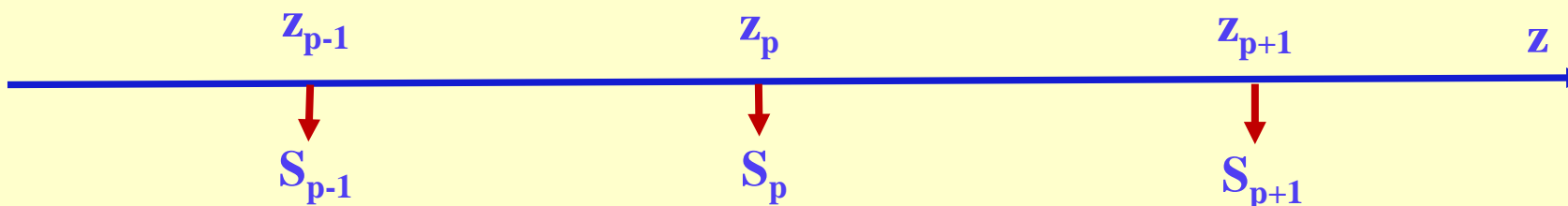
- **Vacuum tightness!**
- **Mechanical stability against external pressure or quenching**
- **Low SEY & PEY: Electron Clouds (EC) problems in case of high intensity positively charged beams**
- **Impedance: LF** - resistive instability (LHC, FCC), **HF**: wake-field at connections, longitudinal non-uniformity, roughness, oxide layer (SuperKEKB at KEK, XFEL at DESY)
- **Power absorption: SR, EC, Image Current**

Phenomena in LHC cold beam pipe



Phenomena in cold beam pipe





$$A \frac{\partial n_i}{\partial t} = q_i + q'_i + \frac{\partial \left(u_i \frac{\partial n_i}{\partial z} \right)}{\partial z} - \sum_p S_{pi} \delta(z - z_p) [n_i - n_{pi}] - s_i [n_i - n_{si}] - \sigma_i C_i l \cdot [n_i - n_{ei}] \approx 0$$

Limited by u_i
100 l/s
10000 l/s

re-cycling

$$l \frac{\partial a_i}{\partial t} = \sigma_i C_i l \cdot [n_i - n_{ei}] - q'_i$$

a_i - surface density of phisorbed molecules
 l - perimeter of the beam pipe cross-section

$C_i = \frac{1}{4} g$

$\sigma_i = f(a_1 \dots a_i \dots a_k, T)$ - Sticking probability
 $n_{ei} = g(a_1 \dots a_i \dots a_k, T)$ - Ultimate density

$$q_i = \eta_i \dot{\Gamma} + \beta_i I_e + \sum_j \psi_{ij} I_j \quad \quad q'_i = \eta'_i(a_i) \dot{\Gamma} + \beta'_i(a_i) I_e + \sum_j \psi'_{ij}(a_i) I_j$$

$\dot{\Gamma}, I_e, I_j$ - fluxes of photons, electrons and ions correspondingly

$\eta_i, \beta_i, \psi_{ij}$ - primary desorption yields at irradiation by photons, electrons and ions correspondingly

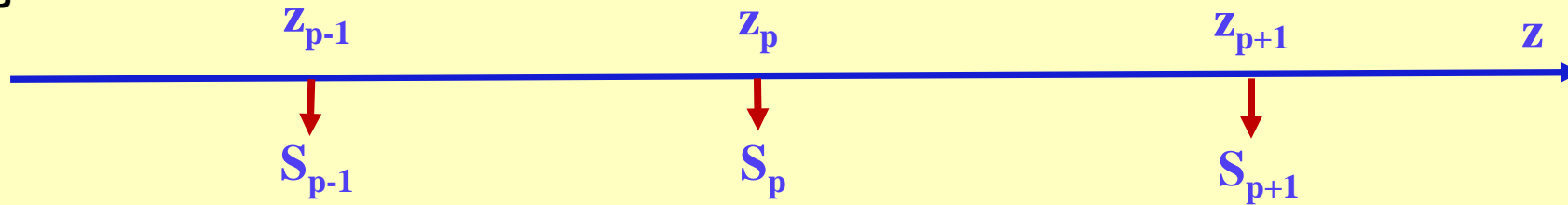
$\eta'_i, \beta'_i, \psi'_{ij}$ - secondary desorption yield (re-cycling)



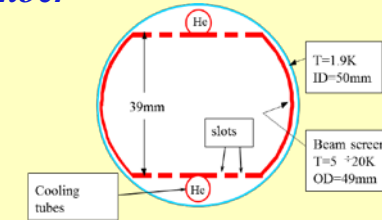
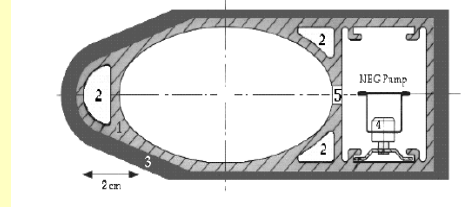
BINP

Equations for residual dynamic gas density prediction

a.a.krasnov@inp.nsk.su



Cross section of the LEP vacuum chamber



LHC

$$A \frac{\partial n_i}{\partial t} = q_i + q'_i + \frac{\partial \left(u_i \frac{\partial n_i}{\partial z} \right)}{\partial z} - \sum_p S_{pi} \delta(z - z_p) [n_i - n_{pi}] - s_i [n_i - n_{si}] - \sigma_i C_i l \cdot [n_i - n_{ei}] \approx 0$$

Limited by u_i

100 l/s

10000 l/s

re-cycling

$$l \frac{\partial a_i}{\partial t} = \sigma_i C_i l \cdot [n_i - n_{ei}] - q'_i$$

a_i - surface density of phisorbed molecules

l - perimeter of the beam pipe cross-section

$$C_i = \frac{1}{4} g$$

$\sigma_i = f(a_1 \dots a_i \dots a_k, T)$ - Sticking probability $n_{ei} = g(a_1 \dots a_i \dots a_k, T)$ - Ultimate density

$$q_i = \eta_i \dot{\Gamma} + \beta_i I_e + \sum_j \psi_{ij} I_j$$

$$q'_i = \eta'_i(a_i) \dot{\Gamma} + \beta'_i(a_i) I_e + \sum_j \psi'_{ij}(a_i) I_j$$

$\dot{\Gamma}, I_e, I_j$ - fluxes of photons, electrons and ions correspondingly

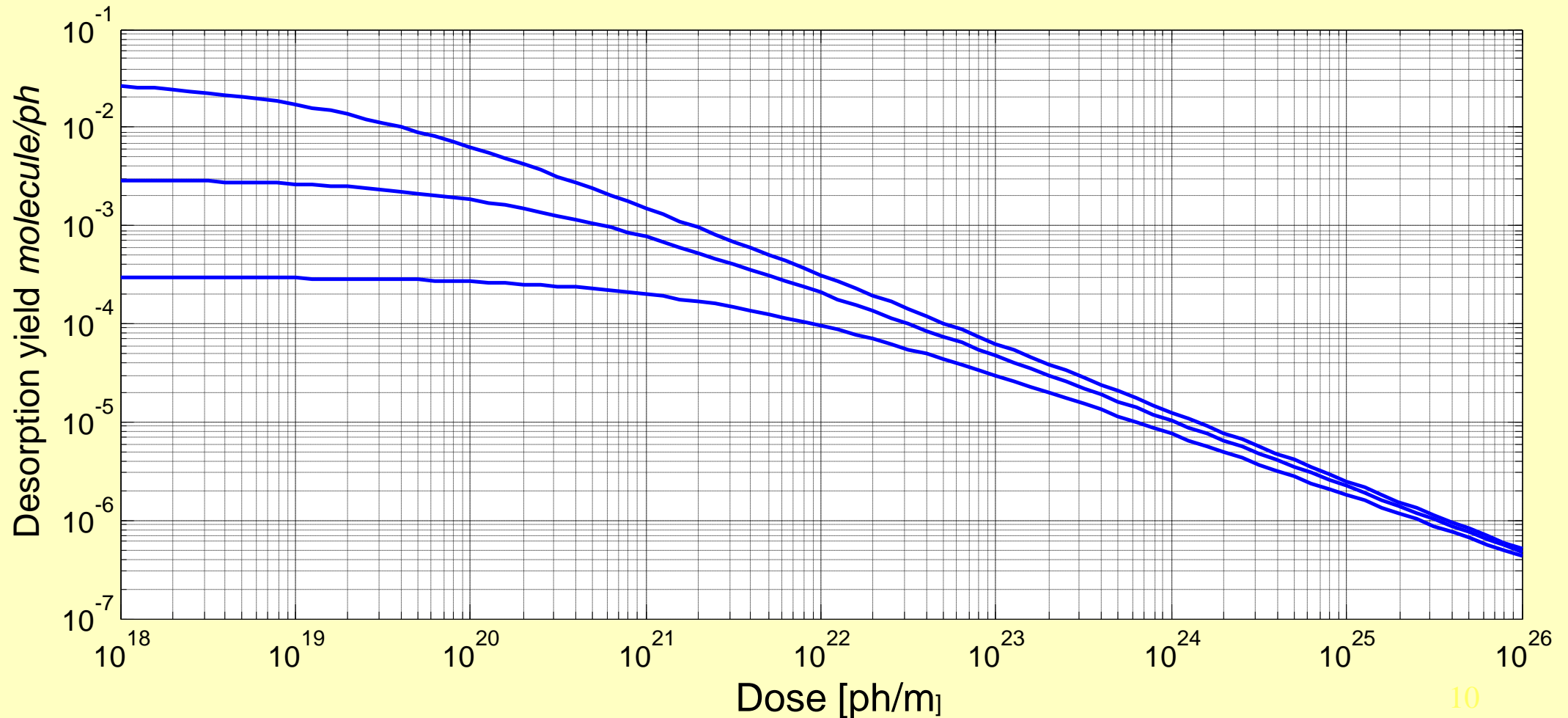
$\eta_i, \beta_i, \psi_{ij}$ - primary desorption yields at irradiation by photons, electrons and ions correspondingly

$\eta'_i, \beta'_i, \psi'_{ij}$ - secondary desorption yield (re-cycling)

Photon stimulated desorption at RT

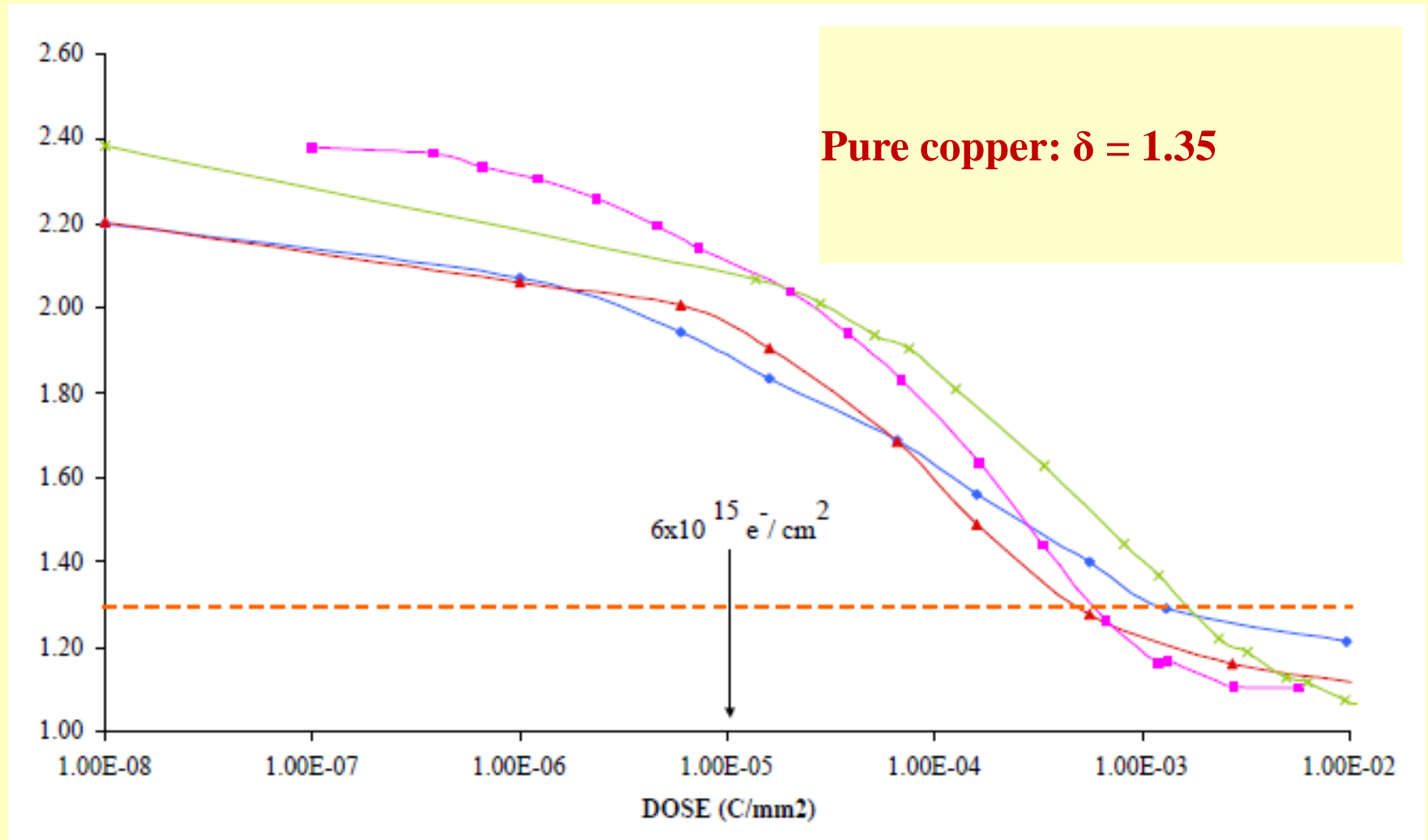
Electron stimulated desorption 30 – 100 times higher

$$\eta = \eta_0 \frac{1}{1 + \left(\frac{\Gamma}{\Gamma_{1/2}} \right)^\varepsilon}$$

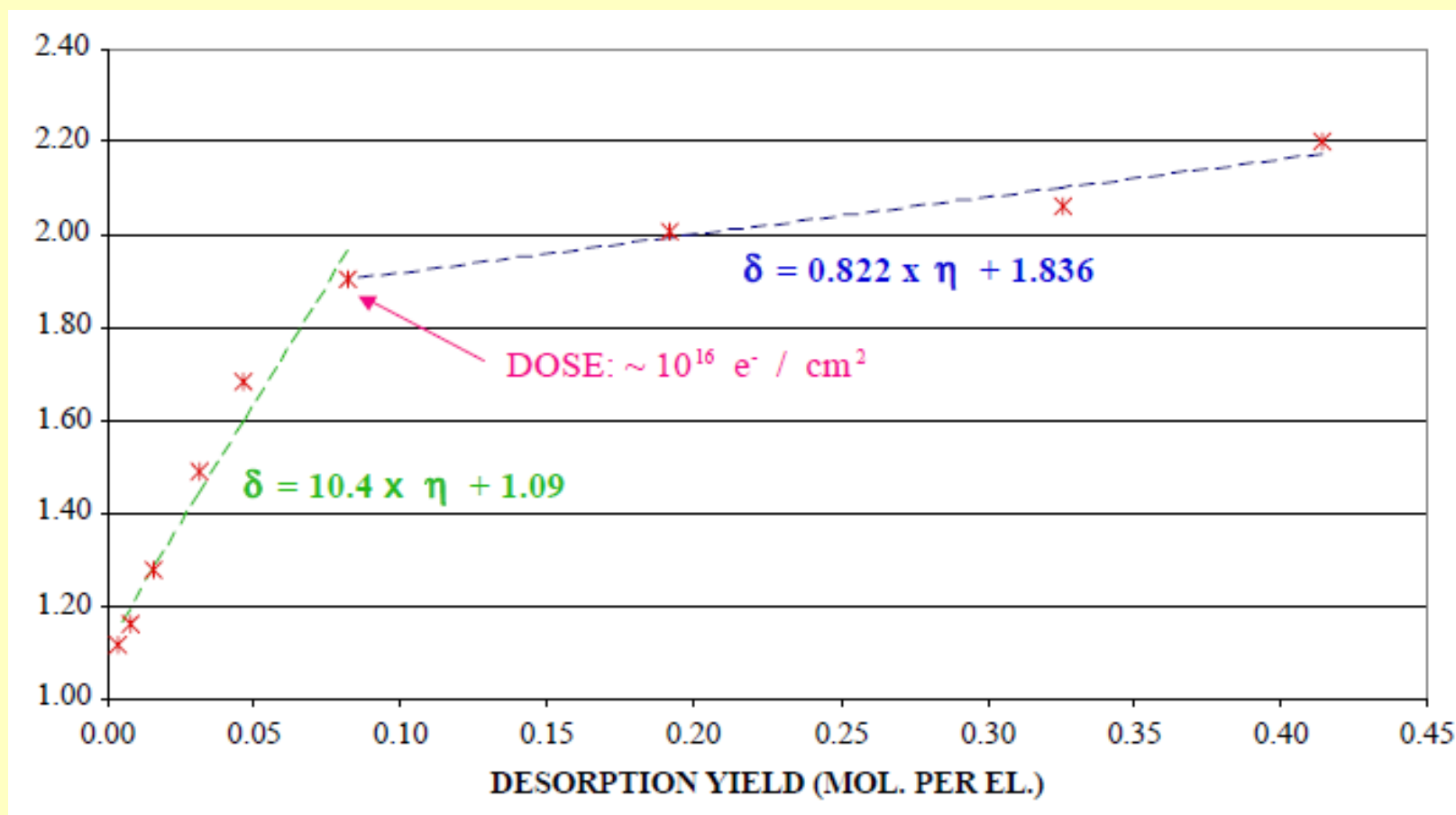


Surface conditioning (SEY must be less 1.3 for LHC arcs)

SEY measurements at CERN for copper samples:



Relation between SEY and ESD during conditioning!



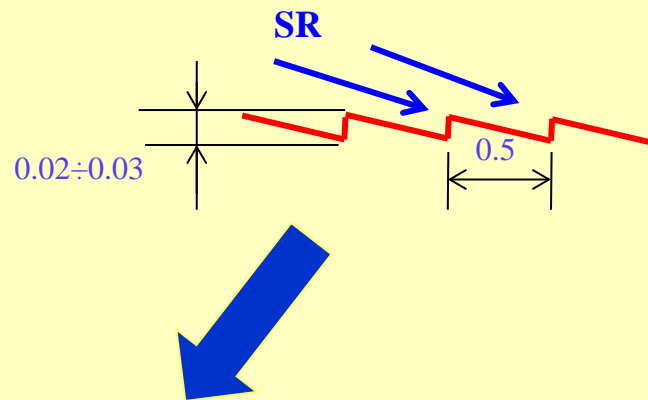
B.Henrist, N.Hilleret, C.Scheuerlein, M.Taborelli, G.Vorlaufer. The variation of the secondary electron yield and of the desorption yield of copper under electron bombardment: origin and impact on the conditioning of the LHC. Proceedings of EPAC 2002, pp. 2553-2555, Paris, France.

Important solutions made for LHC arc beam pipe

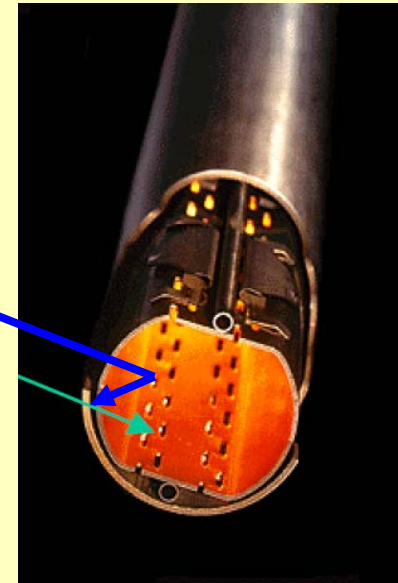
Beam screen: shading of CB against SR and EC, power absorption

Copper co-lamination: high electrical conductivity at cryogenic temperature

Saw tooth!



Slots



Decreasing number of diffusely scattered photons

- decreasing number of photo-electrons ($3 \div 5$ times!) and increasing of conditioning effectiveness

Open question: conditioning is slow in compare with laboratory experiments (10 times at least!)

	LHC	HL-LHC	HE-LHC	FCC h-h	CEPC
Energy per beam, [TeV]	7	7	16,5	50	
Dipole field, [T]	8.4	8.4	20	16	
Current per beam, [A]	0.584	1.12	0.478	0.5	
Bending radius, km	2.8	2.8	2.8	10.4	
SR critical energy [keV]	0.044	0.044	0.575	4.3	
Beam pipe horizontal half aperture [cm]	2.3	2.3	~1.3	~1.3	
SR photon flux in arc [ph/m/s]	1E17	1.8E17	1.9E17	1.6E17	
SR incident angle in arc[mrad]	2.5÷5	2.5÷5	2.5÷5	~1.4	
SR max power in arc [W/m]	0.22	0.425	5.6	36	

Main problems for FCC:

- The SR power absorption
- The chose of the Beam Screen optimum temperature
- Long term prediction of the dynamic gas density

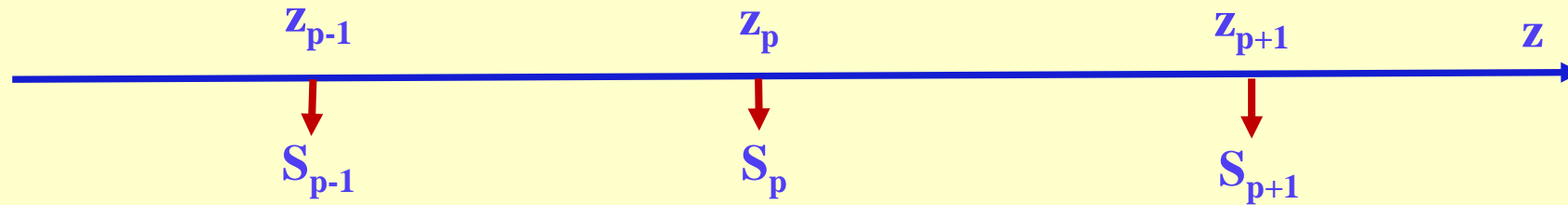
BINP is installing special SR beam line for vacuum investigations

There is experimental program for HL-LHC and preliminary program for FCC

CEPC conceptions of cold beam pipe are welcome to BINP for investigation!

Low cross-section RT beam pipe

(narrow gap undulators, low emittance SR Sources)



$$A \frac{\partial n_i}{\partial t} = q_i + q'_i + \frac{\partial \left(u_i \frac{\partial n_i}{\partial z} \right)}{\partial z} - \sum_p S_{pi} \delta(z - z_p) [n_i - n_{pi}] - s_i [n_i - n_{si}] - \sigma_i C_i l \cdot [n_i - n_{ei}] \approx 0$$

Limited by u_i
~~**100 l/s**~~
~~**10000 l/s**~~

Example: u is in the range $1 \text{ l/s} \cdot \text{m}$, $L = 5 \text{ m}$ $\dot{\Gamma} > 10^{18} \text{ ph/m}$

Even at low $\eta = 10^{-6} \text{ molec/ph}$ (about one year conditioning),

corresponding equilibrium gas density is $n \approx \frac{\eta \dot{\Gamma} L^2}{12u} 10^{-3} \approx 2 \cdot 10^9 \text{ cm}^{-3}$

Or $P \approx 10^{-5} \text{ Pa}$ **after 1 year operation!**



Equations for residual dynamic gas density prediction

a.a.krasnov@inp.nsk.su

Diagram illustrating the spatial distribution of gas density and the corresponding equations for residual dynamic gas density prediction.

The spatial axis z is marked with points z_{p-1} , z_p , and z_{p+1} . The corresponding gas density values are S_{p-1} , S_p , and S_{p+1} .

The governing equation for the gas density n_i is:

$$A \frac{\partial n_i}{\partial t} = q_i + q'_i + \frac{\partial \left(u_i \frac{\partial n_i}{\partial z} \right)}{\partial z} - \sum_p S_{pi} \delta(z - z_p) [n_i - n_{pi}] - s_i [n_i - n_{si}] - \sigma_i C_i l \cdot [n_i - n_{ei}] \approx 0$$

The term $\sum_p S_{pi} \delta(z - z_p) [n_i - n_{pi}]$ is limited by u_i .

The term $s_i [n_i - n_{si}]$ is crossed out with a red X, indicating it is not applicable for the current context.

The term $\sigma_i C_i l \cdot [n_i - n_{ei}]$ is associated with the **NEG coating!** (Non-Evaporable Getter coating).

The term $q_i + q'_i$ is associated with **re-cycling**.

The term $\sigma_i C_i l \cdot [n_i - n_{ei}]$ is associated with **Sorption capacity 1 ML. Lifetime ?**

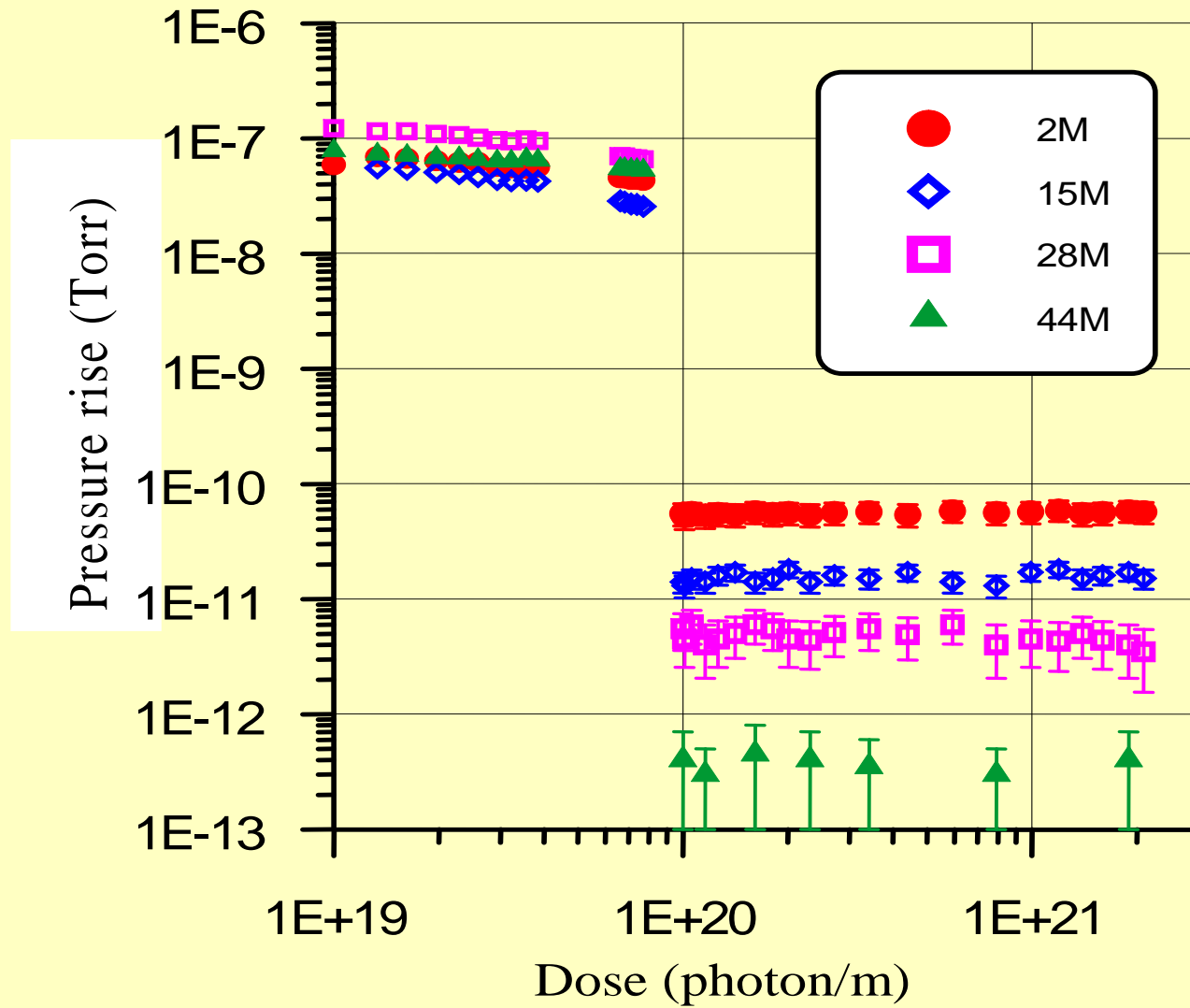
Flow rates are indicated: **100 l/s** (crossed out) and **10000 l/s**.

Most popular **NEG** composition is **TiZrV** – low activation temperature **180 °C**

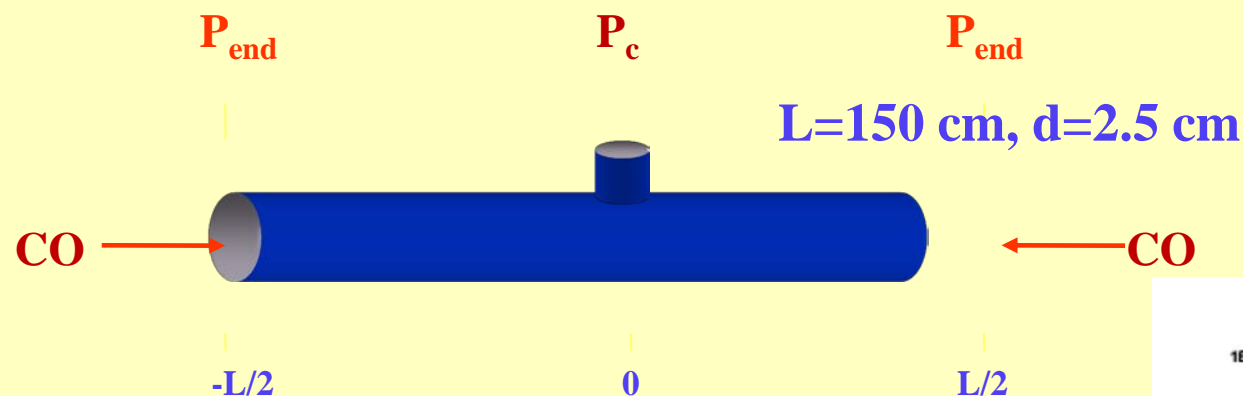
Advantages: **low** $\eta_i, \beta_i, \psi_{ij}$ **and low SEY**, high pumping speed

Disadvantages: **Needs baking**, low sorption capacity (lifetime ?)

Investigation of TiZrV.

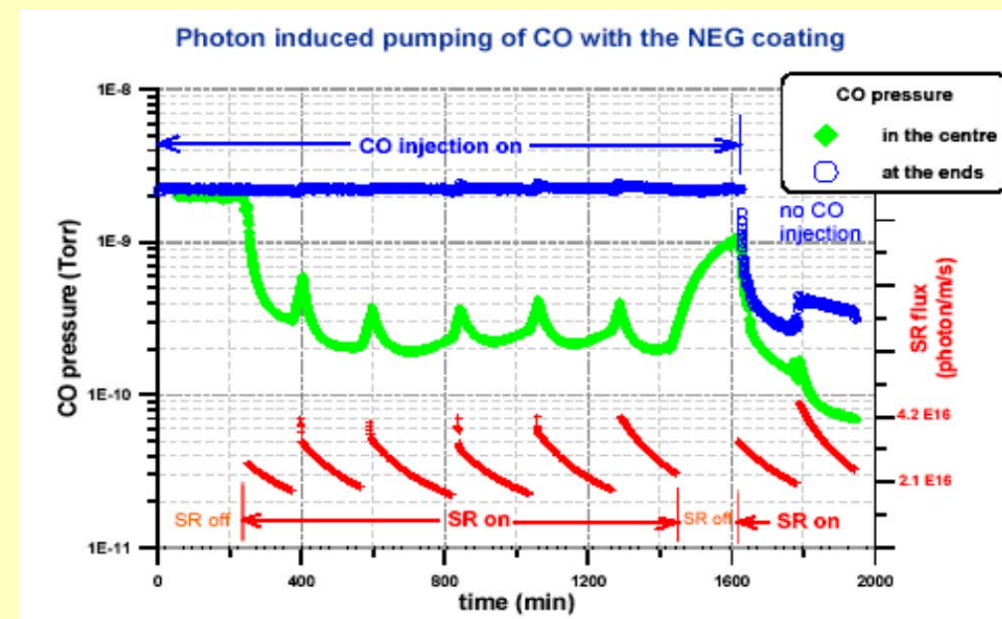
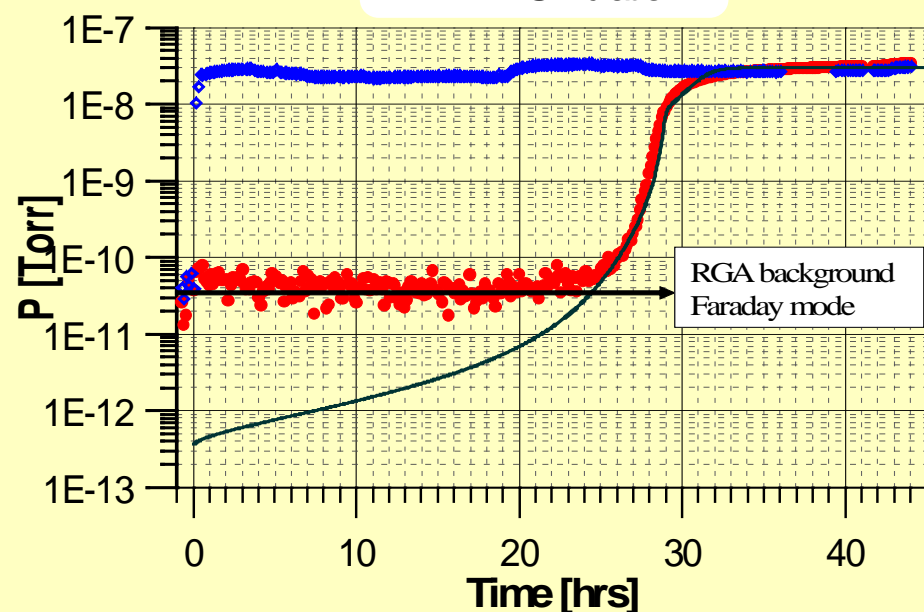


Effect of activation. Photon flux 4E16 ph/m/s



CO saturation

- ◆ CO at edges
- CO at centre
- Simulation



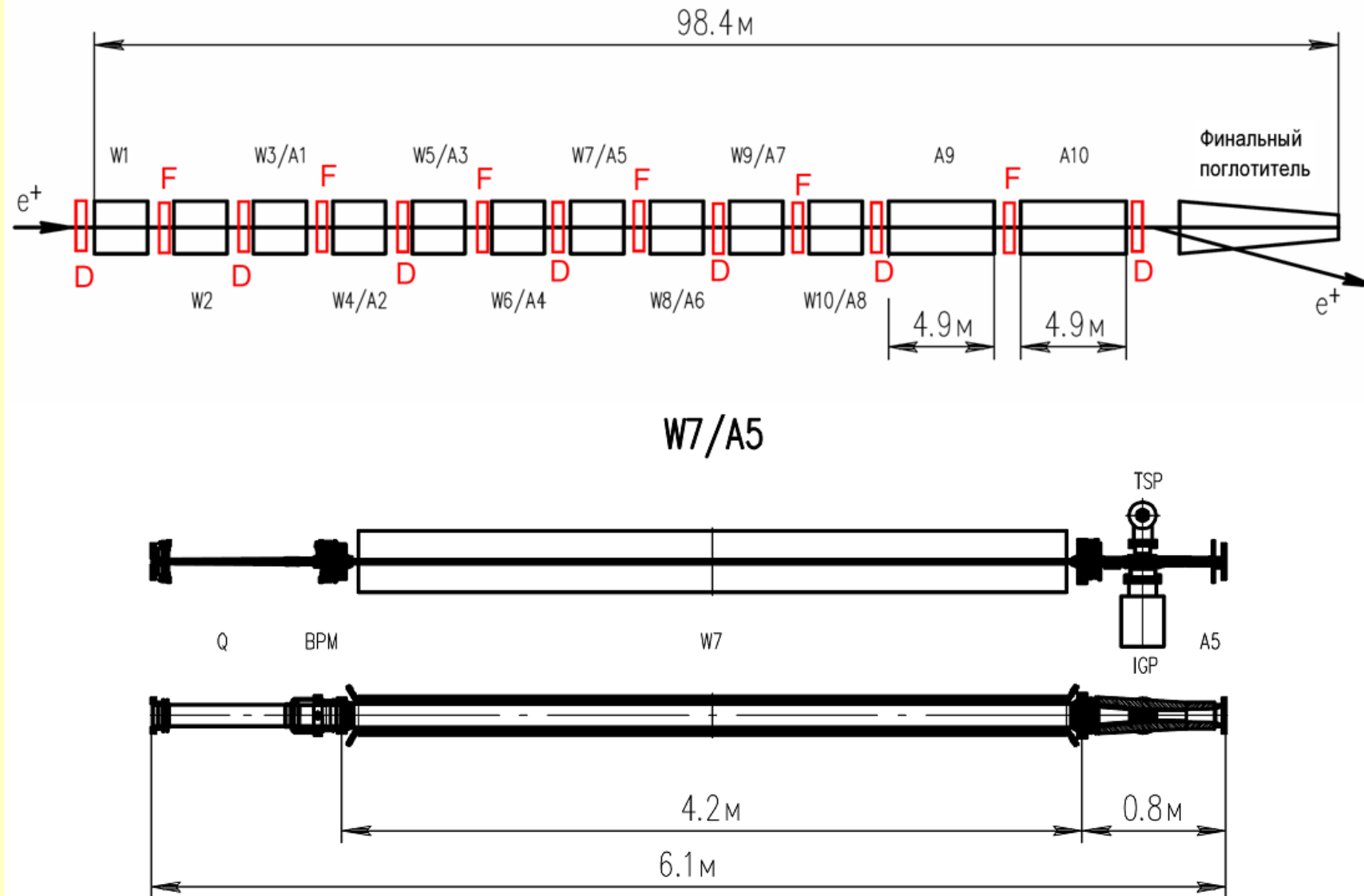
SR stimulate diffusion of molecules into NEG film!

– prolongation of lifetime!

- No re-cycling!

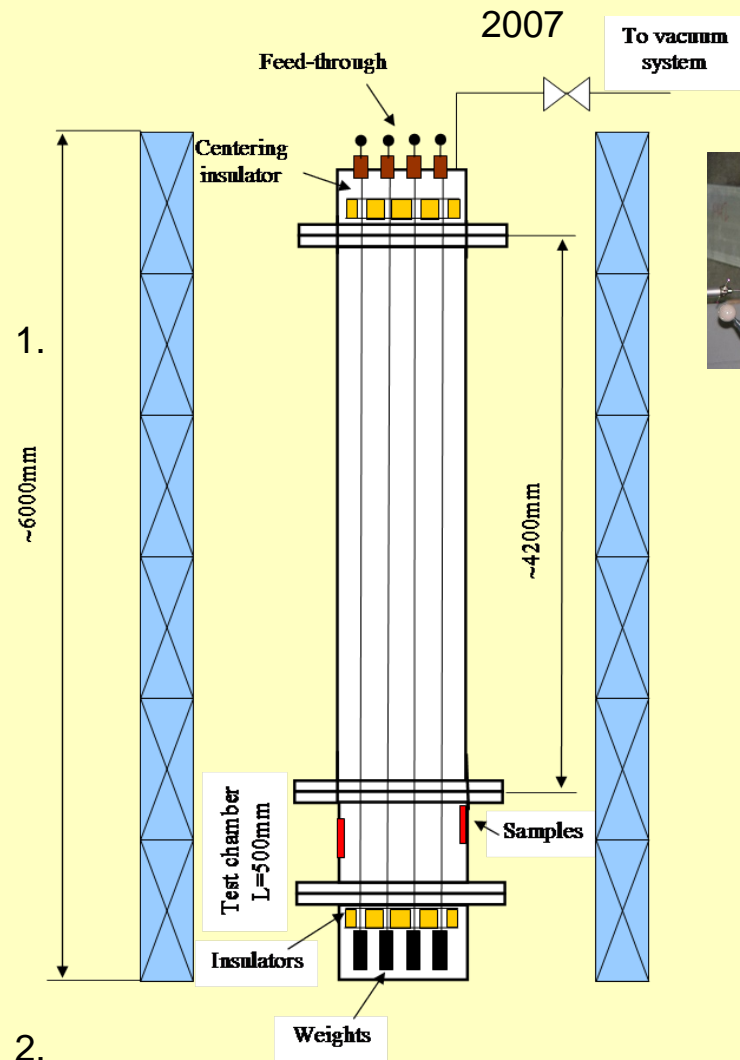
3.3 DWG PETRA III

Total SR power 2×450 kW . $P < 2E-6$ Pa





NEG deposition system



$B_{\max}=700\text{G}$
 $E=200-300\text{ V}$
Power = 10 -15 W/m



Fig.1 Sputtering-deposition system

4 PETRA III damping section wiggler chambers are deposited by TiZrV NEG film

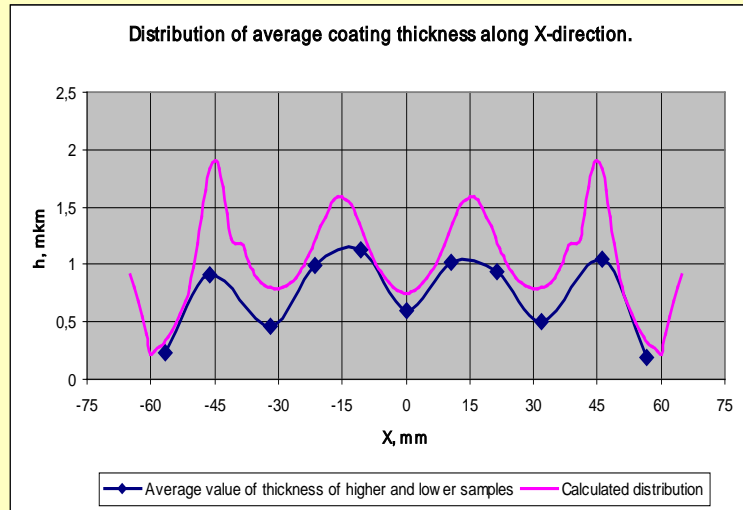


Fig.4. Distribution of average coating thickness along X-direction at Z = 2410 mm.

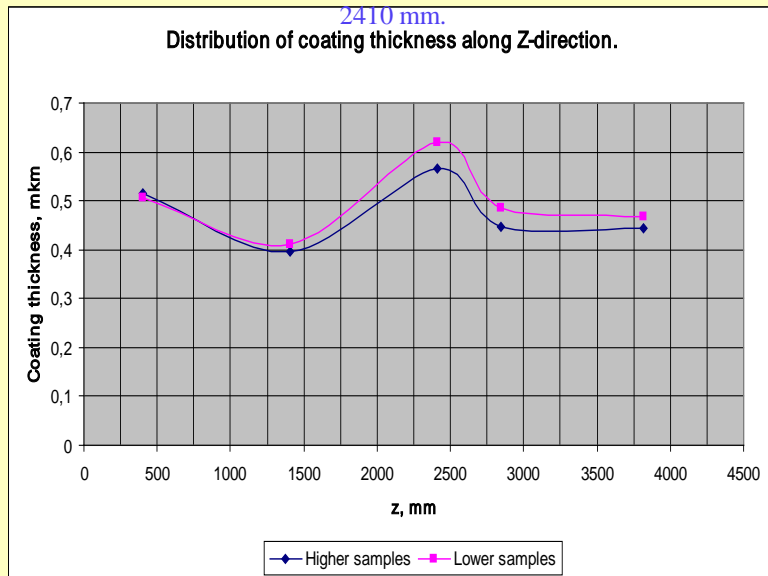


Fig.5. Distribution of coating thickness along Z-direction at X = 0 mm.

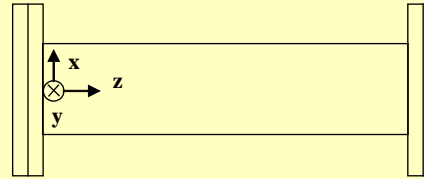


Fig.3. Sketch of the vacuum chamber.

	Weight composition, %	Atomic composition, %
Ti	25	30.4
Zr	32	20.4
V	43	49.2

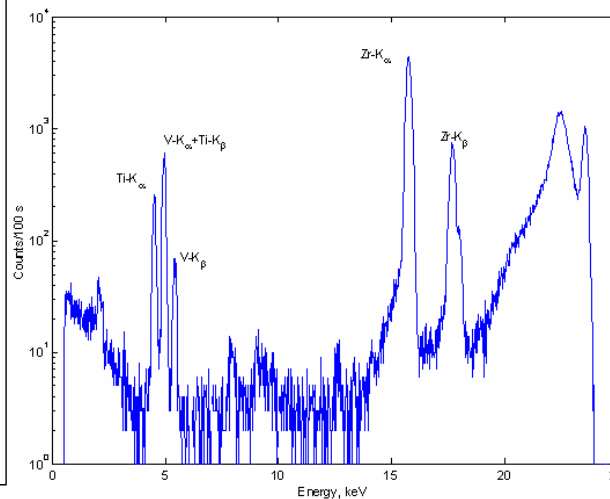


Fig.2. An example of XRF spectrum of getter sample.

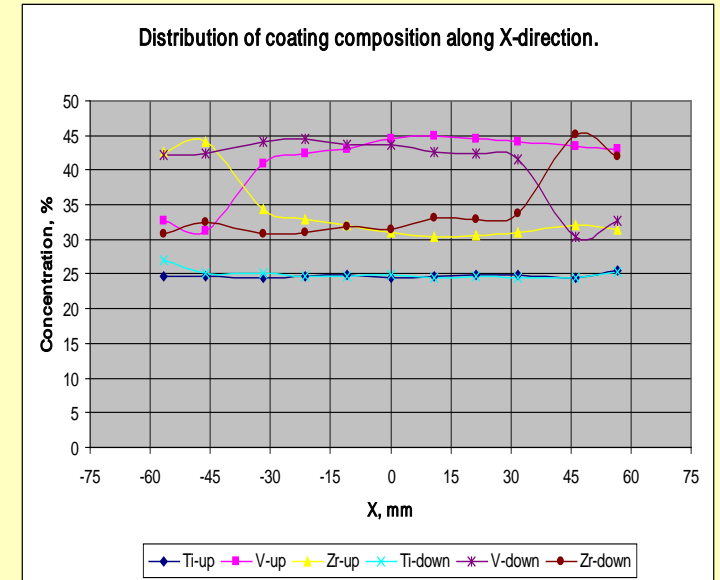


Fig.6. Distribution of coating weight composition along X-direction at Z = 2410 mm.

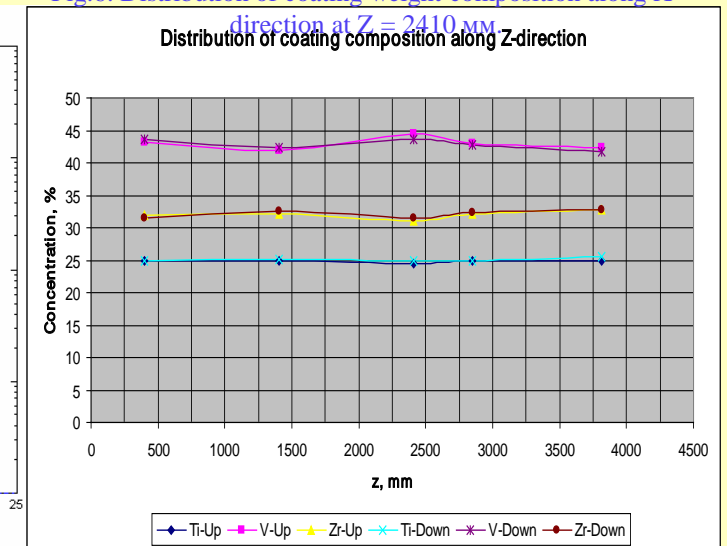
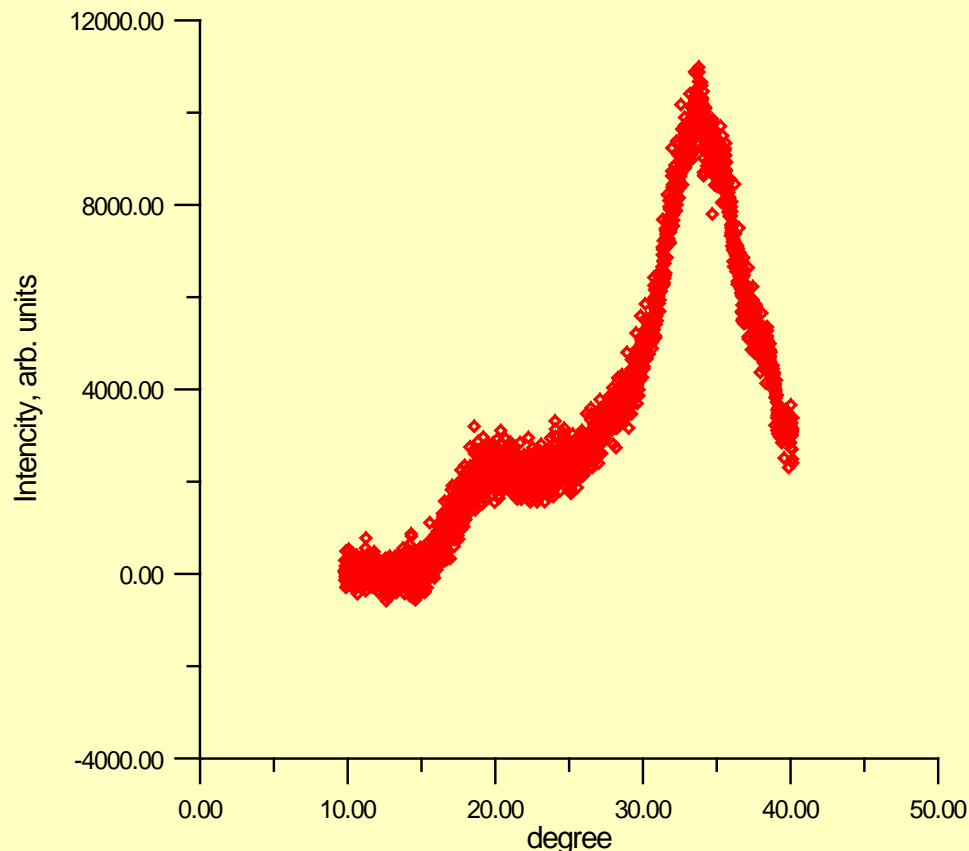


Fig.7. Distribution of coating weight composition along Z-direction at X = 0 mm.

X-Ray Diffraction (XRD) analysis

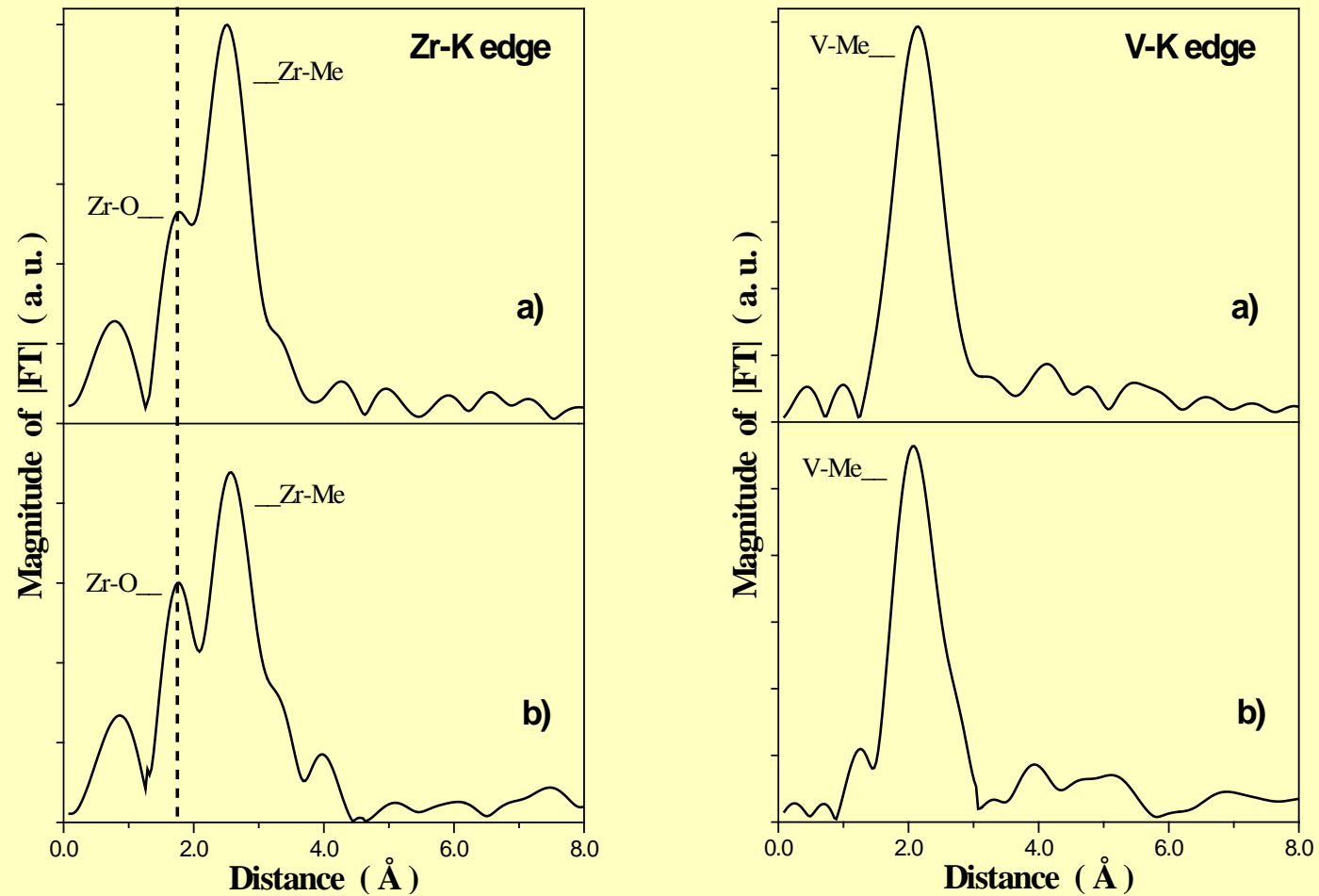


$E_{ph}=8.048$ keV

Substrate is amorphous pure quartz

The XRD pattern of coating seems to be typical for amorphous materials or for materials with very small particle size, not more than ~1.0-1.5 nm.

EXAFS



**FT| curves describing zirconium and vanadium
local arrangement: a) fresh getter; b) old getter**

EXAFS preliminary layout

- Local coordination around Zr and V atoms of the fresh sample seems to be typical for that of metallic glasses. Indeed only one main peak corresponded to the first Me-Me distances is observed at |FT| curves of Zr and V spectra, around 2.5 and 2.2 angstroms, respectively. The values of Me-Me distances taken from |FT| curves are not physical ones, because they are not phase-corrected. The calculated correct values of bond length from Zr and V to the nearest neighbours correspond to 2.9 and 2.7 angstroms, respectively. Taking into account that the difference in metallic radii of Zr and V is also about 0.2 angstroms, one may conclude that the local atomic compositional coordination is uniform. It is also support the metallic glass model of the getter structure.
- Local coordination around Zr of the “old” sample considerably differs from the freshly deposited sample. A small peak at 1.6 angstroms seen at |FT| curve of fresh sample strongly increased in the case of old sample. This peak corresponds to Zr-O bond and reflects the formation of zirconium oxide at the getter surface under atmospheric conditions. As can be seen in Fig.7, the vanadium does not show any traces of oxidation in the freshly prepared sample. Even for the case of the aged sample the vanadium does not considerably oxidized. The magnitude of the peak at 1.3 angstroms, corresponding to V-O bond in |FT| curve, is very small compared to the main V-Me peak. It means that the only Zr atoms capture oxygen under atmospheric conditions.
- The potential of EXAFS spectroscopy for studying of the local atomic structure of ZrTiV NEG is not limited by this study. In future one may to study the changes in structure of NEG under their treatment and working cycles. In this case one may useful to increase the surface sensitivity of EXAFS method by means of the total electron yield (TEY) and (or) other well-known experimental techniques.



Thanks for your attention

